J Mater Sci (2012) 47:3415–3428
DOI 10.1007/s10853-011-6189-x

Vibrational investigation of indigo–palygorskite association(s) in synthetic Maya blue

Constantinos Tsiantos · Maria Tsampodimou · George H. Kacandes · Manuel Sánchez del Río · Vassilis Gionis · Georgios D. Chryssikos

Received: 29 August 2011 / Accepted: 6 December 2011 / Published online: 20 December 2011

Abstract A systematic investigation of the controversial association between indigo and palygorskite in Maya blue (MB), the famous Mesoamerican nano-hybrid pigment, is presented. It is based on vibrational spectroscopy up to near-infrared frequencies, as well as on X-ray diffraction and thermogravimetric analysis. The vibrational data point to a unique vibrational signature of the associated indigoid species over a broad range of experimental parameters (different octahedral composition of palygorskite, indigo concentration up to ca. 10 wt%, preparation temperature up to ca. 130 °C). This signature of MB includes bands attributed to the fundamental, combination, and overtone modes of N–H groups and proves that the associated species is indigo and not dehydroindigo. The high-wavenumber position of the N–H modes suggests that indigo is interacting weakly with the host matrix. The association with palygorskite proceeds with a log(time) kinetic law, provided that the tunnels of the clay are free from zeolitic H_2O. It is found that palygorskite with pre-dried tunnels forms MB even at ambient temperatures. On the contrary, palygorskite with pre-folded tunnels does not associate with indigo. These data are compatible with models involving the diffusion of indigo inside the tunnels of palygorskite. By filling the tunnels, indigo blocks their rehydration at ambient as well as their folding at higher temperatures. At ca. 220 °C, indigo in MB assumes quantitatively a different bonding arrangement. This high-temperature structural transformation of MB is slowly reversible upon rehydration at ambient and its onset is observed at relatively low temperatures (≥130 °C). Thus, MB synthesized above ca. 130 °C and not given sufficient time to rehydrate fully at ambient would still contain variable amounts of the high-temperature species, which may explain conflicting reports about the nature of the guest molecule.

Electronic supplementary material The online version of this article (doi:10.1007/s10853-011-6189-x) contains supplementary material, which is available to authorized users.

C. Tsiantos · M. Tsampodimou · V. Gionis · G. D. Chryssikos (✉)
Theoretical and Physical Chemistry Institute, National Hellenic Research Foundation, 48 Vassileos Constantinou Ave., 11635 Athens, Greece
e-mail: gdchryss@eie.gr

G. H. Kacandes
Geohellas S.A, 8A Pentelis Str., 17564 Athens, Greece

M. Sánchez del Río
European Synchrotron Radiation Facility, BP 220, 38043 Grenoble Cedex, France

Introduction

Maya blue (MB) is the term coined in 1942 by Gettens and Stout [1] to describe a vibrant turquoise-blue pigment in pre-Columbian Mesoamerican murals and artifacts, which differed from anything known in the ancient world and had an unusual durability to weathering and chemicals (for a recent review on the MB pigment, see [2]). Study in the early 1960s by Gettens [3] and Shepard [4] indicated that archeological MB involves palygorskite (a whitish and not particularly acid-resistant clay mineral with a tunnel structure, then called attapulgite) and the organic dye indigo, $C_{16}H_{10}N_2O_2$ (Fig. 1). In 1966, Van Olphen [5] synthesized a material with the same pigment and chemical properties by heating mixtures of palygorskite and synthetic indigo. He found that other common clays do not produce chemically resistant pigments by the same procedure, with the exception of sepiolite which is structurally

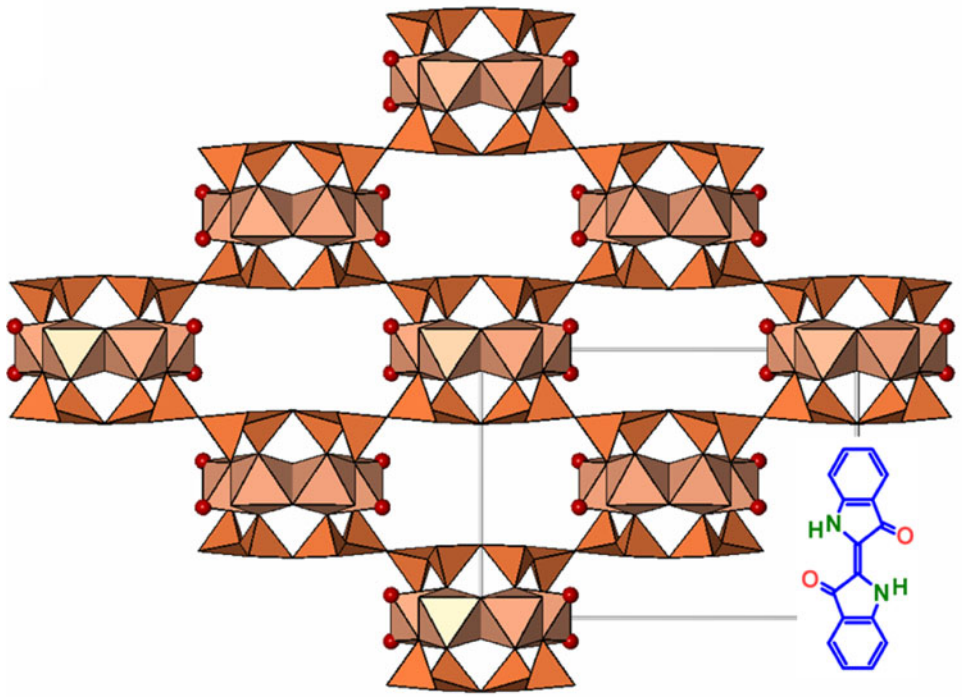

Fig. 1 Schematic cross-section (ca. 35 × 45 Å^2) of a palygorskite lath-like particle, perpendicular to the *c*-axis. Note the periodic inversion of the tetrahedral sheets and the discontinuity of the octahedral sheet resulting in the formation of discreet modules linked by Si–O–Si bonds, zeolitic tunnels, and surface steps. SiOH groups terminate the silicate sheets at the external particle surface. Mg-coordinated OH_2 species lining the side walls of the tunnels are shown as *spheres*. H_2O molecules decorating the inner and outer surface of palygorskite at ambient are not shown. Palygorskite has a variable octahedral composition, which has a small effect on unit cell parameters but does not affect the chemistry of the tunnel walls. Sepiolite (not shown) has an analogous structure with 50% wider modules and tunnels. One molecule of indigo is drawn approximately to scale

analogous to palygorskite. Van Olphen discussed various possibilities for a chemical description of the pigment and concluded that MB is an "adsorption complex of indigo molecules on surface sites specific to palygorskite and sepiolite" [5]. One year later, Kleber et al. [6] published the first infrared spectroscopic study of synthetic MB. Though not conclusive, this study was the first to report that the synthesis of MB involves the dehydration of palygorskite and is accompanied by changes in the spectrum of indigo.

For the next 30 years, MB remained mostly a topic of ethnoarchaeology- or archaeometry-motivated research culminating with the book of Reyes-Valerio [7]. The materials aspects of MB remained dormant until it was described as an "ancient nanostructured material" in a 1996 high resolution TEM study on archeological samples by José-Yacamán et al. [8] Since then, the structural/chemical description of this unusual pigment remains controversial despite efforts.

It is accepted that the formation of MB involves some kind of molecular interaction between indigo (or its oxidized form, dehydroindigo, $C_{16}H_8N_2O_2$) and some kind of structural feature of the clay, which must be specific to the palygorskite–sepiolite family of clays. Several possibilities have been proposed, often combined, all stemming from the unusual structural features of palygorskite [9–11] (Fig. 1); indigo enters the tunnels of palygorskite [12–17], or sits on surface grooves [5, 14, 18], or guards the entrance of the tunnels [17, 19]. Its association with palygorskite may involve H-bonding with the Mg-coordinated OH_2 species lining the inner surface of the clay tunnels [12, 13, 20, 21], or the displacement of OH_2 and the direct chelation to the outer cations of the discontinuous octahedral sheet [16, 22], or bonding to the abundant surface SiOH groups which terminate the tetrahedral sheet [19]. According to other groups [16, 22–27], a significant fraction of indigo in MB, perhaps up to 40% [23], is claimed to convert to dehydroindigo, which then interacts with the clay in one of the aforementioned ways. Alternatively, the interaction of indigo with Fe-containing nanoparticles in palygorskite [8, 28], or with Al^{3+} occupying inner or outer surface sites [16, 22, 25] have been proposed to account for the hue and brilliance of the pigment. In contrast to views which refer to a unique or preferred type of guest–host association, MB has been described also as "a complex system in which different topological isomers of various indigoid molecules attached to the palygorskite matrix coexist" [29].

Vibrational spectroscopy, especially Raman [21, 22, 26, 30–36] and to a lesser extent mid-infrared [6, 21–23], has been employed to identify MB and to study the nature of the indigo–palygorskite association. But, despite reasonable consensus on the vibrational signature which is common to both synthetic and archeological MB, spectral interpretations vary. For example, the presence or absence of N–H groups which would determine whether the palygorskite-associated species is indigo ($C_{16}H_{10}N_2O_2$) or dehydroindigo ($C_{16}H_8N_2O_2$) depends critically on uncertainties in interpreting the vibrational spectra [22, 26, 33].

In a 2009 publication by Sánchez del Río et al. [36], MB was studied by several experimental techniques including in situ monitoring of its formation by synchrotron powder-XRD and Raman spectroscopy, as well as ex situ measurements of attenuated total reflectance in the mid-infrared, near-infrared spectroscopy, and microporosity. This study demonstrated that (a) the formation of MB and the zeolitic dehydration of the tunnels of palygorskite occur over the same temperature range (70–130 °C), (b) the spectrum of palygorskite in MB is identical to that of neat palygorskite subjected to the same thermal treatment, and (c) increasing amounts of palygorskite-associated indigo make the tunnels inaccessible to rehydrating H_2O, but have no effect on the rehydration of the surface SiOH. These data support models which involve the molecular insertion of the dye in the tunnels of palygorskite. However, the important question concerning the possible conversion of indigo to dehydroindigo was not convincingly resolved.

Subsequent important articles on the nature of the palygorskite–indigo interactions in MB include Dejoie et al. [37] reporting on synthetic palygorskite MB with up to 10 wt% indigo. On the basis of thermogravimetric analysis (TGA) and synchrotron X-ray diffraction data, these authors concluded that indigo diffuses inside the tunnels of palygorskite replacing zeolitic H_2O and stabilizing the room-temperature structure of the clay. Ovarlez et al. [38] also studied high indigo content mixtures by mid-infrared spectroscopy and TGA. They reported the formation of two distinct indigo–clay complexes, one involving H-bonding between indigo and the Mg^{2+}-coordinated OH_2 inside the tunnels and the other (formed at higher temperatures and long-living upon re-exposure to ambient) implying direct bonding between Mg^{2+} and the guest molecule.

Parallel to the aforementioned studies of Dejoie et al. [37] and Ovarlez et al. [38], this study is a follow-up of the study by Sánchez del Río et al. [36] and provides the first detailed account of the near-infrared (NIR) spectra of synthetic MB. NIR spectroscopy is the technique-of-choice for detecting subtle structural details of palygorskite, such as those related to its chemical composition [39, 40] and the changes accompanying its dehydration [41, 42]. In Ref. [36], this technique was used to study the state of palygorskite in MB and to monitor surface and tunnel rehydration upon exposure of the freshly made MB to the ambient. In this study, we report specifically on the NIR spectrum of the organic component in MB, assign several of its key features on the basis of the corresponding fundamentals and discuss them in the context of the existing models for the formation of MB. In addition, we investigate whether the octahedral composition of palygorskite affects its ability to form MB, we define the maximum uptake of indigo by palygorskite and monitor the kinetics of MB formation as a function of temperature. Further, we demonstrate the room-temperature synthesis of MB by separating the dehydration of palygorskite from the association of indigo. The article concludes with a preliminary vibrational and thermogravimetric study of MB in the high-temperature range (200–300 °C) known for the folding of the palygorskite structure due to the collapse of its tunnels [9, 11, 43] and related to the appearance of the high-temperature indigo–palygorskite association [38].

Experimental section

Materials and sample preparation

Indigo, $C_{16}H_{10}N_2O_2$, powder was purchased from Fluka and used without further treatment. Most of the MB preparations were based on a palygorskite clay specimen from Ticul (Yucatán, Mexico) which is the same as that employed in the earlier study of Sánchez del Río et al. [36]. Additional experiments were based on palygorskite PFl-1 (Clay Mineral Society source clay, Gadsden County, Florida, USA), SEG (Segovia, Spain), and ESQ (Esquivias, Madrid, Spain) from M. Suárez–E. García-Romero collection, as well as five GRx samples from the authors' collection (Pefkaki deposit, Ventzia basin, W. Macedonia, Greece). All of these samples have been characterized extensively by X-ray diffraction, analytical electron microscopy, vibrational spectroscopy, and other techniques, and reported in the recent literature [39, 41, 42, 44, 45].

The typical synthesis of MB involved heating the hand-ground mixtures of palygorskite and indigo in 0.5–1 g batches. The indigo content is expressed in mg/100 mg clay equilibrated to ambient conditions (ca. 25 °C, 35–40% RH). The mixtures were heated in flat-bottom colorless borosilicate vials (25-mm diameter). Upon completion of the heat treatment (typically 24 h at 130 ± 3 °C unless otherwise indicated), the vials were sealed immediately and left to cool to ambient. Kinetic experiments were performed in the same manner at various fixed temperatures between 70 and 145 °C, and over total heating times of up to 200 h. Room-temperature synthesis of MB in a

liquid medium involved the thermal pre-treatment and cooling of neat palygorskite (300 mg), followed by the addition of dry CCl_4 (20 mL) and the appropriate amount of indigo (ca. 10 mg). The chemical durability of several MB preparations was tested by Soxhlet extractions in $CHCl_3$.

Characterization techniques

NIR data (4000–8000 cm^{-1}) were collected on a Fourier transform instrument (Vector 22N by Bruker Optics) with an Au-coated integrating sphere module. The vials containing the powders were placed directly on the quartz window of the sphere and measured at ambient temperature against an Au-mirror reference. Typical spectra are averages of 200 scans at a resolution of 4 cm^{-1}. Fourier transform was computed using a Blackman-Harris 3-term apodization and a zero-filling factor of 2. The 2nd derivative of the NIR absorption was computed via the Savitzky–Golay subroutine of the OPUS software (Bruker Optics) with 13-point smoothing.

Raman spectra were measured on a dispersive Raman microscope (Renishaw inVia Reflex) equipped with Ar^+ ($\lambda_0 = 488$, 514.5 nm) and diode ($\lambda_0 = 785$ nm) lasers for excitation. The latter are combined with 2400 and 1200 lines/mm gratings, respectively. Samples (ca. 1 mg) were placed in cylindrical aluminum holders and measured at ambient temperature with a ×20 objective. A sealed or purging high-temperature cell (Linkam THMS 600) with a controller (TMS 94) and a fused silica window was employed for Raman measurements up to 300 °C. Complementary mid-infrared spectra were recorded on a Fourier transform spectrometer (Equinox 55 by Bruker Optics) equipped with a single reflection diamond ATR accessory (Durasampl IR II by SensIR). These were typically averages of 100 scans at a resolution of 2 cm^{-1}.

Thermogravimetric traces were recorded on a TGA Q500 analyzer (TA Instruments). The 10 ± 1 mg samples were equilibrated to 40 °C and then scanned to 400 °C at 10 °C/min, under dry N_2 purging (60 mL/min).

Powder X-ray diffraction data were obtained on a Thermo ARL diffractometer (X'TRA 17) with Cu-Kα radiation (45 kV, 40 mA), divergence and receiving slits of 0.4 and 0.5 mm, respectively, and a Peltier detector. Scans were performed from 2° to 70° 2θ with a 0.02° step and a 10 s count time.

Results

The NIR spectrum of indigo in MB

The 2nd derivative NIR spectra of palygorskite exhibit well-defined peaks over three discrete NIR ranges (4000–4900, 5100–5400, and 6900–7300 cm^{-1}) owing to the structural ($\nu + \delta$) OH combinations, the ($\nu + \delta$) H_2O combinations, and the 2ν OH overtone modes, respectively [39, 41]. Significant spectral changes are observed as a result of zeolitic and surface dehydration/rehydration [41, 42]. Regardless of the state of hydration, there remain two nearly transparent windows at ca. 4700–5100 and 5500–6600 cm^{-1} which are suitable for detecting the organic species in both the unheated mixtures and MB preparations. The NIR spectra of pristine YUC palygorskite and mixtures with up to 10 wt% indigo without heat treatment are shown in Fig. 2 (an enlarged version of Fig. 2 is provided in the Electronic supplement as Fig S1a–c). Increasing amounts of (polycrystalline) indigo result in the growing of a well-defined multiplet at 5900–6100 cm^{-1}, accompanied by weak bands at 4847, 4891, and 4969 cm^{-1}. These bands match the NIR spectrum of polycrystalline indigo (Electronic supplement, Fig. S2), and are associated with the C–H stretching overtone and the highest wavenumber portion of the ($\nu + \delta$) combination spectrum of indigo, respectively.

Figure 2 includes also the spectra of the same mixtures after their quantitative transformation to MB by heating to 130 °C. The formation of MB has a very pronounced effect of the NIR signature of indigo. The 2ν CH overtone envelope becomes simpler as the intense 6031 cm^{-1} band of polycrystalline indigo vanishes. The main C–H overtone peaks of MB are observed at 5996 and 5956 cm^{-1}. On the contrary, the combination regime develops a sharp (i.e., strong in the 2nd derivative) quintet at 4789, 4838, 4894, 4921, and 5007 cm^{-1}. This quintet signals the associated indigo in MB. It is several times more intense than the corresponding spectrum of polycrystalline indigo and sufficiently differentiated in wavenumber. Therefore, this quintet is proposed as a new diagnostic for MB, which is valuable for high throughput studies because of the simplicity, accuracy, and reproducibility of data acquisition by Fourier-transform NIR spectroscopy.

The assignment of the combination bands of indigo in the 4700–5100 cm^{-1} range must arise, regardless of its polycrystalline or associated state, from a high-wavenumber fundamental X–H stretching coupled with lower wavenumber modes involving the same X–H species in the 1400–1700 cm^{-1} range. Molecular indigo has a center of symmetry (C_{2h}) and therefore exhibits distinct Raman and infrared-active fundamentals of A_g (R), B_g (R), A_u (IR) or B_u (IR) symmetry. Furthermore, all fundamental modes of indigo above ca. 1150 cm^{-1} represent in-plane vibrations of A_g (R) or B_u (IR) symmetry [33, 46]. Only *ungerade* modes of molecular indigo are active in the NIR [47] and these can only result by combining a Raman-active (A_g) stretching mode with lower wavenumber infrared (B_u) modes or vice versa, since $A_g \times B_u = B_u$. Any combination between two

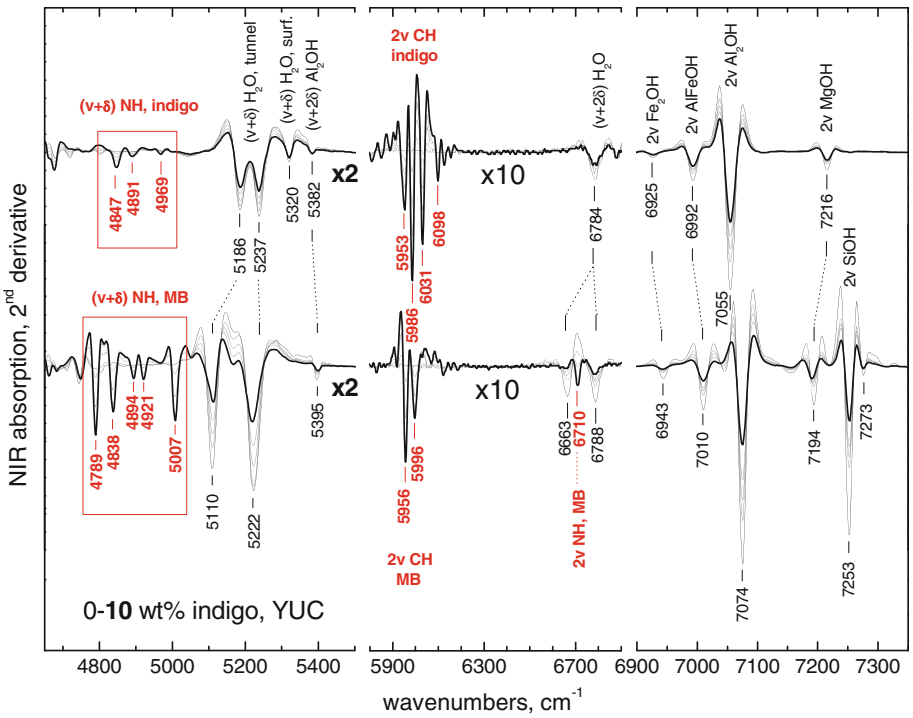

Fig. 2 2nd Derivative NIR spectra of YUC–indigo mixtures with 0, 3, 5, 7, and 10 wt% indigo (*upper*) and their corresponding MB preparations (*lower*). The spectra of the 10 wt% samples are shown in *bold*. For clarity, the derivatives are enhanced by factors of ×10 and ×2 in the 5800–6900 and 4700–5500 cm^{-1} regions, respectively. Assignments for the main bands are included. For details see text. A magnified version of this figure is included in the Electronic supplement (Fig. S1a–c)

modes of the same symmetry yields Raman-active modes ($A_g \times A_g = B_u \times B_u = A_g$). According to this analysis, published infrared and Raman spectra [33, 46, 48] can provide tentative assignments (Table 1) for the weak NIR spectrum of polycrystalline indigo in terms of combinations between, e.g., the infrared-active N–H stretching fundamental (ca. 3270 cm^{-1}) and the Raman-active modes observed at ca. 1585, 1630, and 1700 cm^{-1} (spectra not shown). According to Sánchez del Río et al. [33] and contrary to Tatsch and Schrader [46], the fundamentals at ca. 1585 and 1630 cm^{-1} are assigned a partial δNH character. However, both studies describe the 1700 cm^{-1} mode as a coupled C=O, C=C vibration with no δNH involved. It is remarked that both the articles assign the spectra of polycrystalline indigo on the basis of the predicted modes of molecular indigo. As a result, they do not take into account the intermolecular H-bonding interactions between C=O and N–H in the crystal which are expected to induce some vibrational coupling between their vibrational modes.

By the same token, the mere presence of the 4750–5000 cm^{-1} combination spectrum of associated indigo in MB (Fig. 2, lower) calls for the presence of a hitherto elusive N–H stretching fundamental, while both the intensity and the position of the MB combination bands indicate a significant change of the N–H vibrational energy: The association of indigo with palygorskite and the formation of MB results in the disappearance of the relatively broad N–H stretching mode of indigo at ca. 3270 cm^{-1} and the concomitant appearance of a new sharp band at ca. 3430 cm^{-1} (Fig. 3). This MB band is instrumental for assigning the quintet of NIR-active combination modes of MB (Table 1). The overtone of this N–H band (technically, a combination of the Raman and infrared fundamentals, see above) is observed at 6711 cm^{-1} and increases in intensity with increasing indigo content (Fig. 2, lower).

Blue shifts of N–H stretching fundamentals of similar magnitude are common and explained in terms of decreasing involvement of the N–H to H-bonding associations. For example, the infrared-active N–H stretch of the "associated" (H-bonded) polyamide is observed at ca. 3300 cm^{-1}, while the corresponding mode of "free" N–H is observed at ca. 3450 cm^{-1} and its overtone at ca. 6750 cm^{-1} [49]. Similar high-wavenumber N–H stretching fundamentals and overtones are reported for secondary amides, lactams, anilides, pyrrole etc. in aprotic non-polar solvents [50]. Further, as explained by Siesler [51], the weakening of H-bonding renders the N–H vibration mechanically more anharmonic and therefore more intense in the NIR.

It is noted that a broad band at 3430 cm^{-1} has been reported by Giustetto et al. [21] and assigned to a blue-shifted contribution from the O–H stretching modes of zeolitic H_2O in MB. A closer look at the data in [21] indicates that the heating scheme employed for the preparation of these MB samples (200 °C, vacuum) leads to the folding of palygorskite and is therefore very different to ours.

Table 1 Proposed assignment of the 4800–5050 cm^{-1} NIR spectrum of indigo in the polycrystalline and associated in palygorskite MB states

A_g (R) (cm^{-1})	B_u (IR) (cm^{-1})	$A_g \times B_u$ (NIR) (cm^{-1})	Observed (cm^{-1})
Polycrystalline indigo			
1701	3270	4971	4969
1630	3270	4900	4891
1585	3270	4855	**4847**
3270	1586	4856	
Indigo associated to palygorskite in MB			
1577	3430	5007	**5008**
3428	1584	5012	
1492	3430	4922	4919
3428	1489	4917	
1466	3430	4896	4894
3428	1463	4891	
3428	1409	4837	4837
1362	3430	4792	**4790**

Strongest 2nd derivative bands of diagnostic value are marked in bold

Dependence of the NIR spectrum of MB on palygorskite composition

Most of the published study on synthetic MB is based on palygorskite from Ticul, Yucatan which is rather uniform in composition and structure [45]. Fewer studies [19, 31] are based on palygorskite PFl-1 (CMS standard from Attapulgus, Florida) which is not very different from that of Ticul. However, palygorskite is known to exhibit a broadly variable octahedral composition [44] which can be described by the general formula:

$$y\mathrm{Mg_5Si_8O_{20}(OH)_2(OH_2)_4}\cdot(1-y)$$
$$[x\mathrm{Mg_2Fe_2}\cdot(1-x)\mathrm{Mg_2Al_2}]\mathrm{Si_8O_{20}(OH)_2(OH_2)_4},$$

where x is the fraction of the Fe(III) for Al substitution in dioctahedral palygorskite, and y the fraction of trioctahedral entities [40]. The parameters x and y vary independently from each other and palygorskite samples spanning the ranges $0 \leq x<0.7$ and $0 \leq y<0.5$ have been reported [40]. Notably, this variability in x and y has no effect on the chemical composition of the inner surface of the tunnels, as all the outer octahedral sites of the ribbons are populated by Mg [39].

In addition to YUC (which is defined by $x = 0.12$, $y = 0.07$), we have studied the MB forming ability of eight more palygorskites by heating their mixtures with 5 wt% indigo at 130 °C for 75 h. These are coded SEG (0.01, 0.00), PFL (0.10, 0.06), GR0 (0.36, 0.08), GR1 (0.50, 0.07), ESQ (0.14, 0.33), GR4 (0.60, 0.19), GR7 (0.47, 0.33), and GR9 (0.63, 0.46), where the values in parentheses designate (x, y). Their loci in the triangular diagram of Chryssikos et al. [40] are shown in Fig. S3 (Electronic supplement). Despite spectral differences in the OH overtone and combination regions which result from the variable octahedral composition (Electronic supplement, Fig. S4), all samples exhibit the NIR signature of palygorskite-associated indigo which is characteristic of MB (c.f. Fig. 2, lower).

A close look at the MB-diagnostic combination quintet bands (Fig. 4) reveals that as palygorskite deviates from the ideal dioctahedral composition ($x = 0$, $y = 0$,

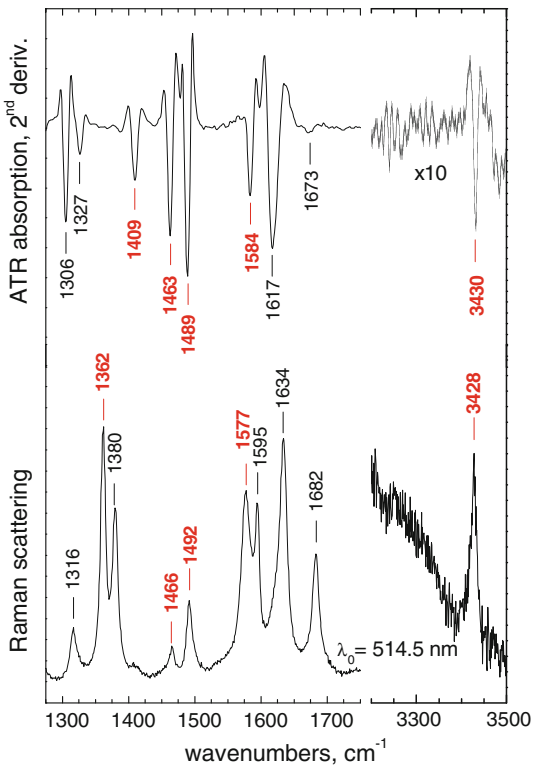

Fig. 3 Detail of the infrared (*upper*) and Raman (lower, $\lambda_0 = 514$ nm) spectra of synthetic MB based on a 7 wt% indigo–YUC mixture. All bands shown are due to the palygorskite-associated indigo in MB, and those marked in *bold* are involved in the proposed assignment of the corresponding NIR spectrum (Fig. 2, Table 1)

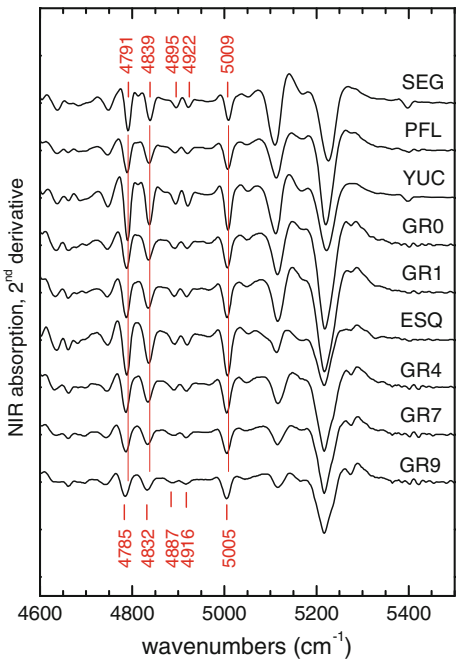

Fig. 4 NIR combination bands of synthetic MB pigments (5 wt% indigo) based on nine different palygorskite samples. The octahedral composition of these palygorskites, their OH overtone signatures, as well as the corresponding ATR spectra in the 1300–1700 cm^{-1} range are shown in Figs. S3–S5 (Electronic supplement)

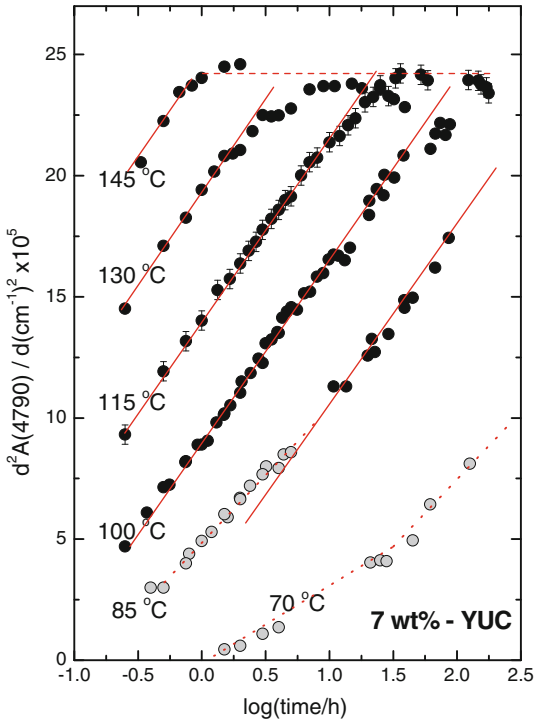

Fig. 5 The time evolution of the absolute intensity of the 2nd derivative NIR spectrum at ca. 4790 cm^{-1} is employed to monitor the formation of MB from a 7 wt% indigo–YUC mixture, as a function of temperature. The *point symbols* indicate the hydration state of palygorskite (*gray*: partially dry; *black*: fully dry) monitored via the position of the AlAlOH stretching overtone. Lines are guiding the eye. Typical error bars in reading the amplitude of the derivatives (applicable to all datasets) are shown

represented by SEG) all five components red-shift by up to 5–6 cm^{-1}. At the same time the bands broaden, thus becoming less intense in the 2nd derivative spectra. Interestingly, the position and width of the fundamental modes of associated indigo in the 1300–1600 cm^{-1} range remain practically unaffected by the composition of palygorskite (see Electronic supplement, Fig. S5). This implies that the exact position and width of the five NIR-active combination bands in MB are defined mainly by the composition dependence of the MB-diagnostic N–H stretch at ca. 3430 cm^{-1}. This is indeed confirmed by Raman spectroscopy (SEG: 3432 cm^{-1}, YUC: 3429 cm^{-1}, GR9: 3423 cm^{-1}, see Electronic supplement, Fig. S6).

Kinetics of MB formation and maximum uptake of indigo

During the course of many NIR measurements of synthetic MB, we found that while for a given palygorskite the intensity of the diagnostic combination bands of associated indigo scale with the amount of indigo, their position, width, and relative intensities remain constant. At the same time, the NIR signature of non-associated polycrystalline indigo is much weaker and does not interfere with that of associated indigo. Under these conditions, the absolute value of the intensity at the deepest 2nd derivative quintet minima (e.g., at 5007 and 4789 cm^{-1}) can be used as a quantitative probe of MB formation. On this basis, the association of indigo with palygorskite can be studied conveniently and systematically as a function of the synthetic parameters (wt% indigo, temperature, and time).

A compilation of such kinetic data for a 7 wt% indigo–YUC mixture is shown in Fig. 5. These data are based on the amplitude of the 2nd derivative 4789 cm^{-1} band but similar results were obtained by probing its counterpart at 5007 cm^{-1}. The data cover the temperature range from 70 to 145 °C and times up to 200 h for the lower temperatures. All measurements are on 500 mg batches at ambient temperature in vials sealed immediately after removing the sample from the furnace. The progress of the indigo–palygorskite association exhibits a sigmoid time dependence which can be fitted neither by a simple diffusion model, nor by one or two exponential terms. Instead, it is linear with log(time) over an extended range of reaction progress (20–90%), therefore exhibiting kinetics of the Elovich type [52].

Obviously, the same NIR spectra which are used for the kinetic study allow for monitoring simultaneously the hydration state of palygorskite. Convenient proxies responding to the presence or absence of zeolitic H_2O in

the tunnels of palygorskite are the positions of the Al_2OH, AlFeOH, Fe_2OH, Mg_3OH modes or the H_2O combination modes, while the SiOH stretching overtones can only be discerned if these surface groups are free from H_2O (Fig. 2, see also [41, 42]). It was observed that the kinetics of indigo association enter the linear log(time) regime when both the surface and zeolitic dehydration processes of palygorskite are complete. At the 500-mg sample scale, this condition is fulfilled for all data at 100 °C and above, as well as for the 85 °C data at times in excess of 10 h (black points in Fig. 5). These data can be time–temperature superimposed over ca. 5 orders of time in hours of which, about 3 orders describe the linear log(time) regime (Electronic supplement, Fig. S7). Lower temperature and/or shorter time data (gray points in Fig. 5) are from palygorskite which is only partially dehydrated and are described by a slower process. An Arrhenius apparent activation energy, $E_a = 1.32 \pm 0.3$ eV (30.4 kcal/mol or 127 kJ/mol), gives the temperature dependence of the association of indigo with zeolitically dry palygorskite in the linear log(time) regime. The time–temperature superposition of the kinetic data indicates that this value of the activation energy is valid over the whole range of reaction (interaction) progress from ca. 20 to 90%.

Mixtures of the same palygorskite with different amounts of indigo, heat-treated at the same range of temperatures, follow the same trace of NIR peak intensity versus log(time), but reach plateaus which depend on the initial indigo content (Electronic supplement, Fig. S7). The intensity of the final plateaus stops increasing above ca. 10–11 wt% indigo. Above this maximum uptake limit of indigo, the observation of the 6031 cm^{-1} C–H overtone band (Fig. 2, upper) persists after very prolonged heat treatments (e.g., 500 h at 130 °C) and indicates the presence of remaining polycrystalline indigo.

High-temperature transformation of palygorskite-associated indigo

A series of YUC-MB preparations with variable amounts of indigo (0–10 wt%, prepared at 130 °C for 24 h and then fully equilibrated at ambient temperature and relative humidity) were studied by thermogravimetric analysis (TGA). The low temperature loss event peaking at 65–75 °C in the derivative traces (Fig. 6) is attributed to the removal of zeolitic H_2O from the tunnels of palygorskite [43]. Upon increasing the content of indigo in MB, this event decreases markedly giving evidence that the tunnels have become inaccessible to rehydration [36]. The same conclusion has been reached on the basis of the TGA data of Chiari et al. [18], Dejoie et al. [37], and Ovarlez et al. [38]. The next loss event (ca. 180–190 °C) is attributed in the case of neat palygorskite to the partial removal

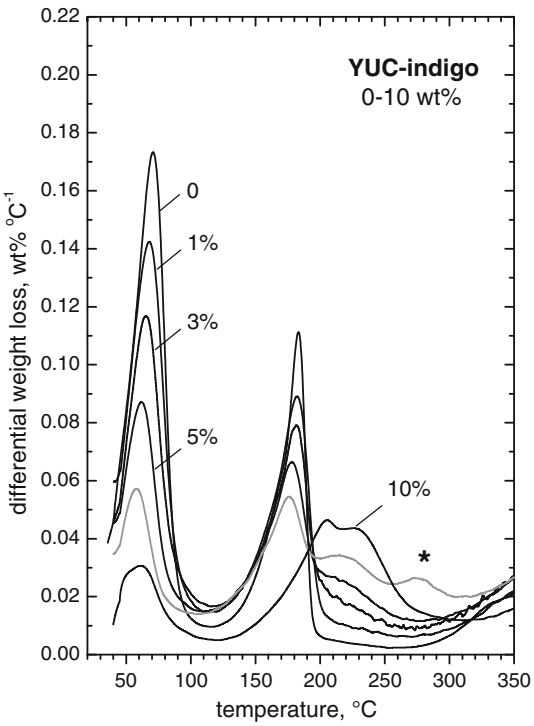

Fig. 6 Differential TGA traces of palygorskite YUC and of YUC-based synthetic MB with 1, 3, 5, and 10 wt% indigo (*solid lines*). The *gray line* corresponds to an incomplete preparation with 10 wt% indigo. The *asterisk* denotes a peak due to the dissociation of unreacted, i.e., non-associated, indigo

of Mg-coordinated OH_2 in the tunnels and the onset of structural folding [43, 53, 54]. As the indigo content of MB increases, we find that the event observed at 180–190 °C is progressively substituted by a higher temperature loss peak at ca. 220–230 °C. The total % loss in the 115–275 °C range remains approximately constant, in agreement with Chiari et al. [18]. We tentatively attribute the new loss peak of MB at 220–230 °C to the removal of coordinated OH_2 in the presence of associated indigo. This assignment is supported by earlier reports that the sublimation of indigo or its dissociation products from MB does not take place until just below 300 °C [18]. These results bear some analogy to those of Ovarlez et al. [38] who measured and compared the TGA traces of MB samples with fixed indigo content (10%) prepared by 30-min isothermal treatments between 120 and 320 °C. Increasing the temperature of the isothermal treatment was found to induce (besides the elimination of zeolitic H_2O) the decrease of the amplitude of the coordinated OH_2 removal event, and possibly its shift to higher temperatures.

To study the influence of the 220–230 °C weight loss event on the spectrum of associated indigo, we measured in situ the Raman spectra of pre-synthesized MB (YUC–10 wt% indigo, $\lambda_0 = 488$ nm) as a function of temperature (130–300 °C). Very pronounced changes of the Raman

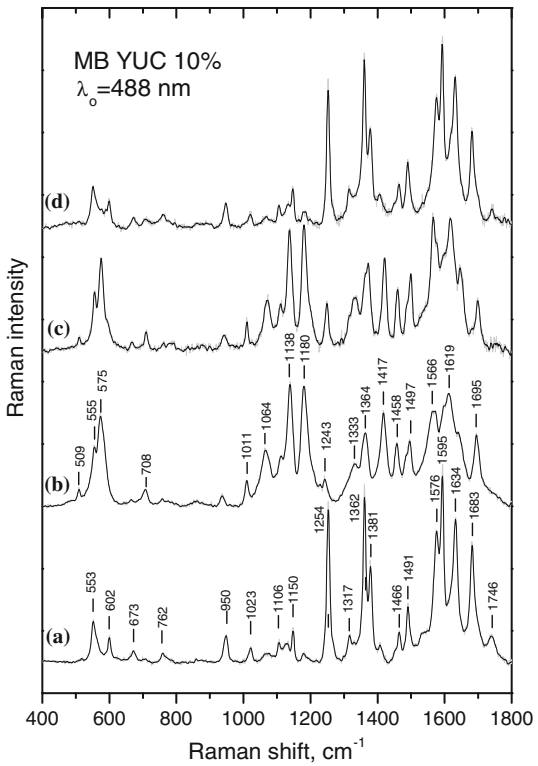

Fig. 7 Raman spectra ($\lambda_0 = 488.5$ nm) of synthetic MB (YUC–10 wt% indigo) at ambient (*a*) and 220 °C (*b*), as well as after heating to 220 °C and cooling to ambient under dry N_2 purging (*c*) or in a sealed cell (*d*)

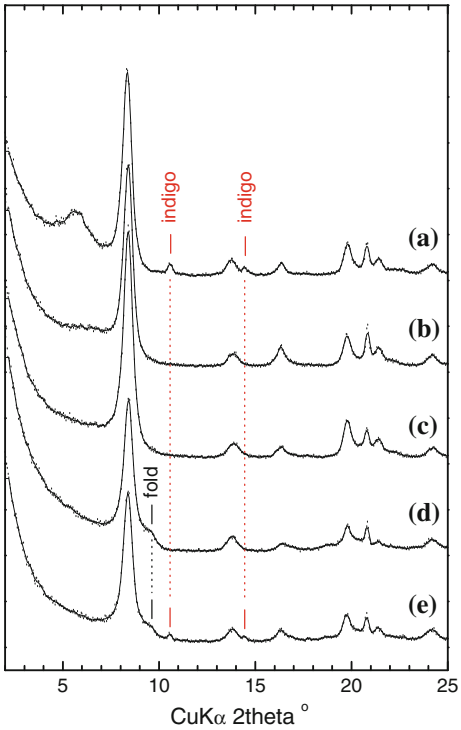

Fig. 8 Powder X-ray diffraction patterns of a palygorskite–indigo mixture (PFL-7 wt%) (*a*), converted to MB by overnight heating at 130 °C (*b*), and then subjected to additional heating at 250 °C for 2 h (*c*). The same palygorskite treated without indigo to 250 °C for 2 h exhibits folding (*d*). Pre-folded palygorskite mixed with 7 wt% indigo and subjected to additional heating at 130 °C for 20 h does not associate with indigo (*e*). Weak sharp bands at ca. $2\theta = 10.5°$ and 14.5° in traces *a* and *e* are due to polycrystalline indigo. The shoulder at ca. $2\theta = 9.5°$ in traces *d*–*e* signals the folding of the palygorskite modules

spectra were discovered. (Fig. 7a, b). These changes involve the broadening and shifting of all Raman bands, as well as the emergence of new peaks, the most prominent of which are at 1417, 1138, and 1180 cm^{-1}. The detailed study of the 2nd derivative Raman spectra as a function of temperature demonstrates that the onset of this high-temperature transformation takes place a little above 130 °C (Electronic supplement, Fig. S8). The transformation becomes quantitative at ca. 220 °C and its product remains stable at least up to 300 °C, regardless of whether heating is performed under air or under N_2. Interestingly, the transformation is fully reversible upon cooling to ambient if the experiment is performed in a closed cell, but irreversible if cooling is performed under a flow of dry N_2 (Fig. 7). This high-temperature structural change is more evident with $\lambda_0 = 488$ nm than $\lambda_0 = 785$ nm excitation (Electronic supplement, Fig. S9), suggesting the importance of Raman resonance effects.

The corresponding ATR and NIR spectra of the MB (YUC–10 wt% indigo) subjected to a high-temperature post-treatment (230 °C, 2 h) are shown in Fig. S10 (electronic supplement) to assist comparisons. These spectra were measured at ambient, immediately following the heating post-treatment. Interestingly, the mid-infrared spectrum of the post-heated MB appears identical to that reported by Ovarlez et al. [38] for 10% indigo–palygorskite mixtures heated to 280 or 320 °C for 30 min.

Aluminous dioctahedral-rich palygorskite (such as YUC or PFL, Electronic supplement, Fig. S3) begin to fold around 200 °C as a result of loosing half of the Mg-coordinated OH_2. In neat palygorskite heated to 250 °C for 2 h, the onset of the folding event is marked by the appearance of a new X-ray diffraction peak at ca. 9.4° 2θ. A similar peak is not observed upon subjecting a 7 wt% MB preparation to the same treatment (Fig. 8). This implies that the association of indigo with palygorskite hinders the collapse of its tunnels, in agreement with Dejoie [17, 37]. Conversely, a pre-folded palygorskite which was mixed with 7 wt% indigo under dry N_2 (to preserve the folded state of the tunnels) and then post-heated to 130 °C (i.e., to conditions suitable for MB formation) does not associate with the indigo which remains polycrystalline (Fig. 8). This latter result is in disagreement with Chiari et al. [18] who reported that heating palygorskite to 350 °C for a few hours and adding polycrystalline indigo before the temperature drops to ca. 100 °C results in the instantaneous

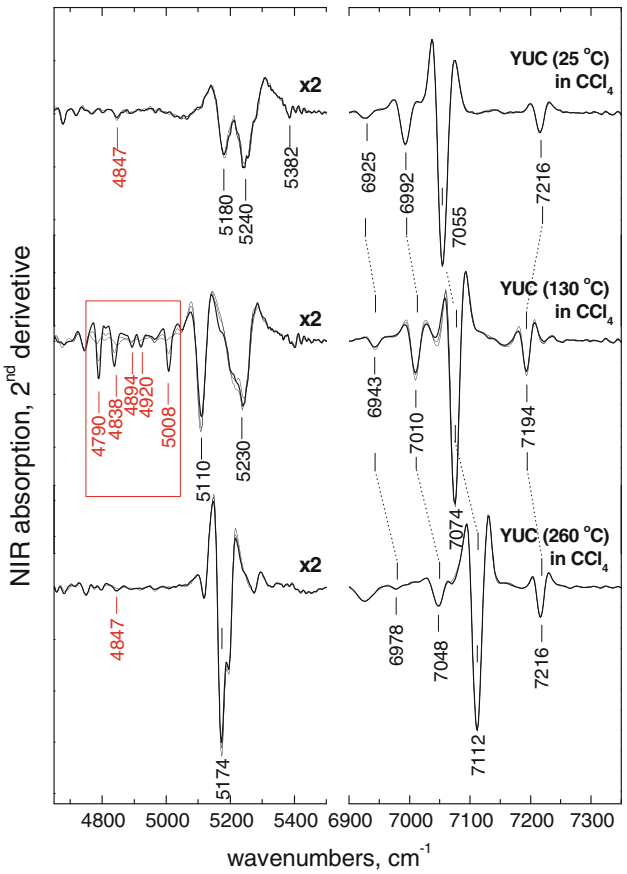

Fig. 9 Details of the 2nd derivative NIR spectra of palygorskite (YUC) precipitated in dry CCl_4 in the presence of ca. 3 wt% indigo. Palygorskite was added to CCl_4 in the as-received hydrated form (*upper*), after being zeolitically dehydrated by heating to 130 °C for 2 h (*middle*), and after folding at 260 °C for 2 h (*lower*). Each set consists of three spectra obtained immediately after the addition of palygorskite, as well as after 5 h and 7 days at room temperature. Spectral intensities are normalized to those of the structural OH stretching overtone bands (6900–7250 cm^{-1}). The association of indigo with palygorskite is observed only in the case of zeolitically dry palygorskite (*middle*) via the characteristic quintet of N–H combination modes (4790–5008 cm^{-1}, c.f. Fig. 2). In systems based on hydrated and folded palygorskite (*upper*, *lower*) indigo does not associate to palygorskite

formation of MB. It is emphasized that experiments testing the MB forming ability of pre-folded palygorskite such as those presented here or reported earlier by Chiari et al. [18] are not comparable to those involving the heating of palygorskite–indigo mixtures to temperatures corresponding to the folding range of the pristine clay [38]. In the latter case, indigo can apparently associate to palygorskite before the folding of its structure can take place, i.e., during or after (high temperature) zeolitic dehydration.

Room-temperature synthesis of MB

The results presented in the last two sections link the formation of MB with the existence of zeolitically dry, but otherwise unfolded and intact, tunnels of palygorskite. This state of the tunnels is achieved by mild heating in the 100–130 °C range. In addition, heating may have an important contribution to the detachment of molecular indigo from its crystal lattice and/or to the activation of its association with the palygorskite host. These processes would be overlapping in the "one pot" synthesis of MB. Higher temperature synthesis will lead to additional complications due to the activation of folding. To resolve better the various processes involved, we have studied the synthesis of the pigment not only from ambient (i.e., zeolitically wet), but also from pre-dried (130 °C for 2 h) and pre-folded (260 °C, 2 h) palygorskite to which ca. 3 wt% indigo was added. Reactions were carried at ambient temperature in tetrachloromethane and studied in situ by NIR. CCl_4 was chosen as the reaction medium for a number of reasons: it lacks C–H bonds and is therefore virtually transparent in the NIR. As a non-polar and nearly spherical molecule, ca. 6 Å in diameter [55], it is not expected to interact significantly with palygorskite, nor penetrate its tunnels. CCl_4 wets but does not disperse palygorskite. Hence, palygorskite settles out in CCl_4 and can be measured conveniently by diffuse reflectance in the NIR through the bottom of the glass container in the presence of the transparent solvent. Finally, indigo is slightly soluble in CCl_4 and, therefore, an equilibrium concentration of molecular indigo is available for associating with palygorskite.

The spectrum of palygorskite in CCl_4 was measured immediately after the addition of indigo and then monitored for a period of ca. 7 days, with occasional shaking. The data (Fig. 9) are shown over the 6900–7350 cm^{-1} (stretching overtones of structural OH) and 4700–5500 cm^{-1} (H_2O and N–H combination modes) ranges, by analogy to Fig. 2. The presence of CCl_4 has no effect on the position and relative intensity of the structural OH modes of ambient and zeolitically dry palygorskite. The positions of the OH overtones of folded palygorskite (Fig. 9, lower) have not been reported previously but are compatible with the published positions of the corresponding fundamentals [53]. Comparison with the spectra of Fig. 2 indicates that, in the presence of CCl_4, the bands attributed to surface H_2O (5320 cm^{-1} in the ambient state) and SiOH terminations (7253 cm^{-1} in the dry state) disappear which suggests that the solvent interacts with the outer surface of palygorskite.

A very weak band at ca. 4850 cm^{-1} which remains invariable as a function of time hints to the presence of polycrystalline indigo in the reaction based on ambient palygorskite (Fig. 9, upper). Indigo in solution cannot be detected. The same 4850 cm^{-1} band of polycrystalline indigo can be seen in the spectrum of the reaction based on zeolitically dry palygorskite immediately after the addition

of indigo, but is seen to convert readily to the characteristic quintet of N–H combination modes in palygorskite-associated indigo (Fig. 9, middle). This is clear evidence for the formation of MB at room temperature (c.f. Fig. 2). Perhaps not surprisingly, no association of indigo with pre-folded palygorskite can be detected (Fig. 9, lower).

Discussion

Convenient data acquisition in the NIR has enabled the study of many MB preparations differing in the provenance (hence, octahedral composition) of palygorskite, the content of indigo (up to ca. 10 wt%), the temperature (up to ca. 130 °C) and the time of heating. Within these broad ranges of independent variables, the synthetic MB exhibits a unique vibrational signature in the NIR. The same signature has been observed at ambient temperature by associating indigo and pre-dried palygorskite in CCl_4.

It is the analysis of this signature that proves the preservation of the N–H moiety in the palygorskite-associated indigo species. The fundamental N–H stretching in MB is identified at ca. 3430 cm^{-1} in both the mid-infrared and Raman spectra and its first overtone is detected in the NIR at ca. 6710 cm^{-1}. These new vibrational features become part of the known vibrational signature of synthetic or archeological MB. The assignments of the fundamental mid-infrared and Raman spectra of indigo in MB appear now better resolved; in qualitative agreement with Sánchez del Río et al. [33], several sharp bands in the 1350–1600 cm^{-1} range involve contributions from N–H displacements, as they are essential in accounting for the observed $(\nu + \delta)$ combination spectra of palygorskite-associated indigo (Table 1). The unusual (though not unprecedented [49–51]) sharpness and high energy of the N–H stretching mode in MB indicates weak or no involvement of this moiety in H-bonding during the association of indigo with palygorskite. Although this weakening is reported by comparison to the dense intermolecular H-bonding pattern of polycrystalline indigo (where each molecule bonds to four neighboring molecules via C=O···H–N interactions [56]), the role of N–H···OH_2 bonding in stabilizing MB [21] appears to be of low or no importance.

The aforementioned data suggest that at least two of the three "uniqueness hypotheses" expressed by Doménech et al. [26, 29] namely that there is a unique organic component in MB and a unique way this is associated to palygorskite, are valid in samples prepared below ca. 130 °C. Furthermore, the single, well-defined type of species which is involved into quantitative association with palygorskite in both synthetic and archeological MB cannot be dehydroindigo because the latter has no N–H bonds. This finding does not exclude the presence of trace concentrations of dehydroindigo or other indigoid species which could influence the visible color or the electrochemical properties of MB while remaining below the detection threshold of vibrational spectroscopic techniques.

The next issue of interest concerns the location of indigo in the inorganic host matrix. Clearly, models involving the association of indigo with minority structural characteristic of palygorskite, such as the ill-documented exposed Al^{3+} sites or the openings of the tunnels, should be abandoned. This is because these models cannot account for the large amount of indigo (up to ca. 10 wt%) associated with palygorskite in a manner described by a unique vibrational signature [17] and also because they imply that MB formation should depend strongly on the composition of palygorskite, which is not observed.

Three possibilities remain: association with surface SiOH groups, fitting in the surface grooves, or sliding inside and filling the tunnels. The first possibility should be excluded because (a) the NIR-active SiOH stretching mode of dry palygorskite remains unaffected in position and intensity after association with increasing amounts of indigo and (b) because the SiOH groups remain accessible to rehydration [36]. The surface groove model was advocated recently by Chiari et al. [18] in a reconsideration of earlier tunnel-filling models by the same group [12, 13, 15]. According to this model, the surface grooves (channels, i.e., incomplete tunnels) offer the same environment for association as the tunnels but, as they are open from one side, they allow for the simultaneous adsorption of many indigo molecules. In contrast, filling the tunnels is inherently a serial process based on one-dimensional diffusion. Chiari et al. [18] argue that the strong H-bonding interactions between the entering indigo molecule and the side walls of the tunnels would impede further movement and result in blocking the entrance of the tunnels. If this was the case, the maximum weight percentage uptake of indigo by palygorskite would have been smaller by about two orders of magnitude [17]. In addition, we should note that Chiari et al. [18] draw the main experimental support for their surface groove model from a questionable interpretation of their TGA data: They claim that the loss of zeolitic H_2O from the tunnels of neat palygorskite occurs in the 150–300 °C range. As the association of indigo in synthetic MB has little effect on the total magnitude of this loss event, the authors conclude that the hydration/dehydration of the tunnels is not affected by the formation of MB. However, several studies combining thermal analysis with structural techniques (XRD, vibrational, and NMR) have demonstrated that zeolitic dehydration takes place below 150 °C and that losses in the 150–300 °C range are due to the removal of coordinated OH_2 which causes the onset of folding [43, 53, 54]. This study has confirmed that the

zeolitic dehydration of the tunnels is a prerequisite for the uninhibited formation of MB. Also, it is the rehydration of the tunnels that becomes hindered by the association of indigo with palygorskite, as seen in both NIR [36] and TGA (Fig. 6, Refs. [18, 37, 38]).

More arguments could be found in favor of the tunnel insertion model and against the association of indigo with surface grooves.

Palygorskite is known [57] to cleave easily along the diagonal [110] plane and, therefore, the external surface profile of its particles is dominated by steps and not grooves, as shown schematically in Fig. 1.

It would have been anticipated that as the grooves are decorated by rows of SiOH terminal groups, the latter would show some perturbation by the neighboring indigo species; this has not been observed in the NIR (Fig. 2, Ref. [36]).

The association of indigo within the surface grooves would leave the guest molecule vulnerable to the perpendicular oxidative attack of the central C=C chromophore by, e.g., nitric acid [17] and would not explain satisfactorily the amazing chemical resistance of MB [58].

In disagreement with Chiari et al. [18], we found that pre-folded palygorskite (i.e., with tunnels collapsed as a result of heating above 250 °C) does not form MB (Figs. 8, 9). In addition, we confirmed the finding of Dejoie et al. [17, 37] who reported that preformed MB does not fold if heated to 250 °C. In other words, the vacancy and accessibility of the tunnels are prerequisites for the association of indigo but, once MB is formed, the tunnels can no longer collapse. The same conclusion has been reached by Ovarlez et al. [59] on sepiolite-based MB.

In the presence of associated indigo, the removal of half of the Mg-coordinated OH_2 from the tunnels is observed ca. 50 °C higher than in neat palygorskite (Fig. 6), suggesting that this process becomes perturbed (perhaps sterically hindered) by the associated guest species.

Both the high wavenumber and sharpness of the N–H mode of the associated indigo in MB and the absence of indigo-induced red-shifts in the $(\nu + \delta)$ H_2O combination modes of zeolitically dry palygorskite (Figs. 2, 3) are signaling weak guest–host interactions. This is opposite to the strong H-bonding association model of Giustetto et al. [21] which was used as an argument in favor of the surface groove hypothesis [18]. Indigo residing inside the tunnels of palygorskite, e.g., in the manner described by earlier studies of Chiari and Giustetto et al. [12, 13], may indeed be much more labile [20] than initially thought.

The kinetic data are valuable in determining the time–temperature conditions for the full incorporation of indigo in palygorskite. At the present level of analysis, the experimentally determined kinetic law does not provide a definite molecular-scale description of the association mechanism [52]. The apparent activation energy ($E_a = 1.32 \pm 0.3$ eV, 30.4 kcal/mol or 127 kJ/mol) is of similar magnitude to the sublimation enthalpy (1.41 eV, [60]) or the calculated lattice energy (−1.38 eV, [61]) of crystalline indigo. This may be suggesting that the rate-determining step in the formation of MB is dominated by the breaking of the intermolecular H-bonding pattern of crystalline indigo and not by the indigo–palygorskite association itself. On the other hand, the logarithmic time dependence of the reaction progress may be describing a highly correlated process which is slower than $t^{1/2}$ diffusion.

So far, this discussion dealt exclusively with the chemistry of a unique type of indigo–palygorskite interaction observed in MB which is synthesized by heating in the ca. 100–130 °C range. Heating polycrystalline indigo and palygorskite over this temperature range is sufficiently high for emptying the tunnels from zeolitic water, for detaching a sufficient amount of molecular indigo from its lattice and for thermally activating its insertion and movement inside the tunnels. At the same time, temperature is not high enough for the release of Mg-coordinated OH_2 and the collapse of the tunnels.

The situation changes dramatically upon treating MB at higher temperatures; the loss of coordinated OH_2 shifts from ca. 200 to 230–250 °C and the vibrational spectra of the associated guest molecule undergo drastic changes (Figs. 7, S9, S10). The process is reversible upon cooling if performed in a closed container, but the high-temperature phase is relatively long-lived at ambient if cooled under N_2 purging and then exposed to ambient humidity. The same high-temperature interaction has been observed by "one pot" high-temperature synthesis (280–320 °C) by Ovarlez et al. [38] who also noted its resistance to rehydration at ambient. Obviously, the nature of the high-temperature MB species is far from being resolved and more studies will be needed for its elucidation. We can, however, speculate that this high-temperature indigo–palygorskite interaction is related to the removal of Mg-coordinated OH_2 species and the establishment of some kind of direct coordination with the side walls of the tunnels leading to the immobilization of the organic guest.

More importantly, we have found that the high-temperature transformation of the associated indigo becomes detectable, albeit in trace quantities, already at 130 °C by 2nd derivative $\lambda_0 = 488$ nm Raman spectroscopy (Electronic supplement, Fig. S8). This demonstrates that more than one indigoids coexist in the tunnels of palygorskite at temperatures between ca. 130 and 230 °C and that some of the high-temperature species may persist upon cooling (depending on synthetic conditions, relative humidity, indigo concentration, and time). In other words, we propose that part of the complexity about the chemical nature of MB as well as the persistent reports for the presence of dehydroindigo may be justified by the variable presence of

the high-temperature indigoid species in the investigated ambient samples combined with the different sensitivity of the analytical techniques employed. Interestingly, Doménech et al. [29] report that the formation of dehydroindigo is favored by increasing temperature, but provide no data allowing for comparison with the high-temperature species reported here and in Ref. [38].

A last comment is deserved about the comparison of palygorskite-based MB with its sepiolite analog, which has its own parallel history of investigations and controversies [5, 19, 58, 59, 62–68]. Sepiolite is similar to palygorskite in terms of structural modulation as well as in outer- and inner-surface chemistry, but its tunnels (and surface grooves) are about 50% wider and 5% taller than those of palygorskite [11, 66] and its folding occurs at ca. 300 °C [43]. The lower chemical durability of sepiolite MB has been reported [58, 65] and attributed to the fact that the structural tunnels are now considerably wider and H bonds can form with only one side of the guest molecule [67, 68]. Despite these differences, the conclusions of the recent XRD, TGA, infrared, NMR, and Heteronuclear Correlation studies of sepiolite MB by Ovarlez et al. [38, 59, 62] and Raya et al. [64] are remarkably similar to those of this study: No interaction of indigo with the external surface of sepiolite has been detected and no evidence for the formation of dehydroindigo is found. Instead, indigo is inserted in the sepiolite tunnels and impedes their folding at high temperatures. At high temperatures, a new type of association between indigo and sepiolite is identified and supposed to involve direct bonding to Mg.

Conclusions

A single indigoid species is identified by vibrational spectroscopy in synthetic MB which is prepared by heating mixtures of palygorskite and indigo in the 85–130 °C range. The vibrational data include the fundamental, combination, and overtone spectrum of N–H bonds, proving that this palygorskite-associated species is indigo and not dehydroindigo. The sharpness and high energy of the N–H spectrum indicate that the indigo–palygorskite association in MB involves weak or no H-bonding via the N–H group. Relatively large amounts of indigo (up to ca. 10 wt%) can be associated with palygorskite in a process that begins with the zeolitic dehydration of its tunnels and then proceeds with a log(time) kinetic law. Palygorskite with pre-dried tunnels can form MB even at ambient temperature, but palygorskite with pre-folded tunnels does not associate with indigo. Once inside the tunnels of palygorskite, indigo blocks their rehydration, perturbs the removal of Mg-coordinated OH_2 species and hinders the folding of the structure at ca. 200 °C. At ca. 220 °C, MB converts quantitatively to a new bonding arrangement and the N–H groups are no more detectable in the vibrational spectra. This structural transformation of MB is slowly reversible upon rehydration at ambient, while its onset is observed at relatively low temperatures ($\geq$130 °C). Further studies of the high-temperature indigo–palygorskite association may rationalize the controversies in the literature of MB concerning the presence of other indigoid guest molecules.

Acknowledgements M. Suárez (U. Salamanca, Spain) and E. García-Romero (U. Complutense, Madrid) are thanked for helpful discussions and for the donation of palygorskite samples SEG and ESQ. N. Theodorakopoulos (NHRF) is thanked for insight about the kinetic data. CT acknowledges C. Raptis (Natl. Technical University of Athens) for encouragement and support. D. Palles (NHRF) and M. Drossos (Geohellas) are thanked for expert technical assistance.

References

1. Gettens R, Stout G (1942) Painting materials, a short encyclopedia. Van Nostrand, New York
2. Sánchez del Río M, Doménech A, Doménech-Carbó MT, Vásquez de Agredos Pasqual ML, Suárez M, García-Romero E (2011) In: Galan E, Singer A (eds) Developments in palygorskite-sepiolite research, developments in clay science 3, Chap 18. Elsevier, mfdh, p 453
3. Gettens RJ (1962) Am Antiq 27:557
4. Shepard A (1962) Am Antiq 27:565
5. Van Olphen H (1966) Science 154:645
6. Kleber R, Messchelein-Kleiner L, Thissen J (1967) Stud Conserv 12:41
7. Reyes-Valerio C (1993) De Bonampak al Templo Mayor: El azul maya en Mesoamerica, Colección America Nuestra, vol 40. Siglo XXI editores, Mexico, DF
8. José-Yacamán M, Rendón L, Arenas J, Serra Puche MC (1996) Science 273:223
9. Singer A (1989) In: Dixon JB, Weed SB (eds) Minerals in soil environments, 1. SSSA book series. Soil Science Society of America, Madison, WI
10. Artioli G, Galli E (1994) Mater Sci Forum 166–169:647
11. Post JE, Heaney PJ (2008) Am Miner 93:667
12. Chiari G, Giustetto R, Ricchiardi G (2003) Eur J Miner 15:21
13. Giustetto R, Chiari G (2004) Eur J Miner 16:521
14. Reinen D, Köhl P, Müller CZ (2004) Anorg Allgem Chem 630:97
15. Giustetto R, Levy D, Chiari G (2006) Eur J Miner 18:629
16. Tilocca A, Fois EJ (2009) J Phys Chem C 113:8683
17. Dejoie C, Dooryhée E, Martinetto P, Blanc S, Bordat P, Brown R, Porcher F, Sánchez del Río M, Stroble P, Anne M, Van Elslande E, Walter P (2010) arXiv: 1007.0818v1 (July 6)
18. Chiari G, Giustetto R, Druzik J, Doehne E, Ricchiardi G (2008) Appl Phys A 90:3
19. Hubbard B, Kuang W, Moser A, Facey GA, Detellier C (2003) Clay Clay Miner 51:318
20. Fois E, Gamba A, Tilocca A (2003) Microporous Mesoporous Mater 57:263
21. Giustetto R, Llabrés i Xamena F, Ricchiardi G, Bordiga S, Damin A, Gobetto R, Chierotti MJ (2005) J Phys Chem B 109:19360
22. Manciu FS, Reza L, Arres L, Chianneli R (2007) J Raman Spectrosc 38:1193

23. Doménech A, Doménech-Carbó MT, Vásquez de Agredos Pasqual ML (2006) J Phys Chem B 110:6027
24. Doménech A, Doménech-Carbó MT, Vásquez de Agredos Pasqual ML (2007) J Phys Chem C 111:4585
25. Polette-Niewold LA, Manciu FS, Torres B, Alvarado M Jr, Chianelli RR (2007) J Inorg Biochem 101:1958
26. Doménech A, Doménech-Carbó MT, Edwards HGM (2011) J Raman Spectrosc 42:86
27. Rondão R, de Melo JSS, Bonifacio VDB, Melo MJ (2010) J Phys Chem A 114:1699
28. Polette LA, Meitzner G, José-Yacamán M, Chianelli R (2002) Microchem J 71:167
29. Doménech A, Doménech-Carbó MT, Sánchez del Río M, Vásquez de Agredos Pasqual ML, Lima E (2009) N J Chem 33:2371
30. Witke K, Brzezinka K, Lamprecht I (2003) J Mol Struct 661–662:235
31. Leona M, Casadio F, Bacci M, Picollo M (2004) J Am Inst Conserv 43:39
32. Vandenabeele P, Bodé S, Alonso A, Moens L (2005) Spectrochim Acta A 61:2349
33. Sánchez del Río M, Picquart M, Haro-Poniatwoski E, van Elslande E, Uc VH (2006) J Raman Spectrosc 37:1046
34. Wiedemann HG, Brziezinka K-W, Witke K, Lamprecht I (2007) Thermochim Acta 456:56
35. Moreno RG, Strivay D, Gilbert B (2008) J Raman Spectrosc 39:1050
36. Sánchez del Río M, Boccaleri E, Milanesio M, Croce G, Van Beek W, Tsiantos C, Chryssikos GD, Gionis V, Kacandes GH, Suárez M, García-Romero E (2009) J Mater Sci 44:5524. doi: 10.1007/s10853-009-3772-5
37. Dejoie C, Martinetto P, Dooryhée E, Brown R, Blanc S, Bordat P, Strobel P, Odier P, Pocher F, Sánchez del Río M, Van Elslande E, Walter P, Anne M (2011) M RS Proceedings, 1319, mrsf10-1319-ww06-01. doi:10.1557/opl.2011.924
38. Ovarlez S, Giulieri F, Delamare F, Sbirrazzuoli N, Chaze A-M (2011) Microporous Mesoporous Mater 142:371
39. Gionis V, Kacandes GH, Kastritis ID, Chryssikos GD (2007) Clay Clay Miner 55:543
40. Chryssikos GD, Gionis V, Kacandes GH, Stathopoulou ET, Suárez M, García-Romero E, Sánchez del Río M (2009) Am Miner 94:200
41. Gionis V, Kacandes GH, Kastritis ID, Chryssikos GD (2006) Am Miner 91:1125
42. Stathopoulou ET, Suárez M, García-Romero E, Sánchez del Río M, Kacandes GH, Gionis V, Chryssikos GD (2011) Eur J Miner 23:567
43. Hayashi H (1969) Am Miner 54:1613
44. García-Romero E, Suárez M (2010) Clay Clay Miner 58:1
45. Sánchez del Río M, Suárez M, García-Romero E (2009) Archaeometry 51:214
46. Tatsch E, Schradder B (1995) J Raman Spectrosc 26:467
47. Bokobza L (2002) In: Siesler HW, Osaki Y, Kawata S, Heise HM (eds) Near-infrared spectroscopy. Wiley-VCH, New York, pp 11–41
48. Tomkinson J, Bacci M, Picollo M, Colognesi D (2009) Vibr Spectrosc 50:268
49. Wu P, Siesler HW (1999) J Near Infrared Spectrosc 7:65
50. Foldes A, Sandorfy AC (1970) Can J Chem 48:2197
51. Siesler HW (2002) In: Siesler HW, Osaki Y, Kawata S, Heise HM (eds) Near-infrared spectroscopy. Wiley-VCH, New York, pp 213–245
52. Landberg PT (1955) J Chem Phys 23:1079
53. Prost R (1975) PhD Thesis, University of Paris VI, France
54. Kuang W, Glenn AF, Detellier C (2004) Clay Clay Miner 52:635
55. Webster CE, Drago RS, Zerner MC (1998) J Am Chem Soc 120:5509
56. Süsse P, Steins M, Kupcik V (1988) Z Kristallogr 184:269
57. Chen T, Wang H, Zhang X, Zheng N (2008) Acta Geol Sin (Eng Ed) 82:385
58. Sánchez del Río M, Martinetto P, Reyes-Valerio C, Dooryhee E, Suárez M (2006) Archaeometry 48:115
59. Ovarlez S, Giulieri F, Chaze A-M, Delamare F, Raya J, Hirschinger J (2009) Chem Eur J 15:11326
60. Cox JD, Pilcher G (1970) Thermochemistry of organic and organometallic compounds. Academic Press, New York
61. Thetford D, Cherryman J, Chorlton AP, Docherty R (2004) Dyes Pigments 63:259
62. Ovarlez S, Chaze AM, Giulieri F, Delamare F (2006) C R Chimie 9:1243
63. Doménech A, Doménech-Carbó MT, Sánchez del Río M, Goberna S, Lima E (2009) J Phys Chem C 113:12118
64. Raya J, Hirschinger J, Ovarlez S, Giulieri F, Chaze A-M, Delamare F (2010) Phys Chem Chem Phys 12:14508
65. Giustetto R, Wahyudi O, Corazzari I, Turci F (2011) Appl Clay Sci 52:41
66. Post JE, Bish DL, Heaney PJ (2007) Am Miner 92:91
67. Giustetto R, Seenivasan K, Bonino F, Ricchiardi G, Bordiga S, Chierotti MR, Gobetto R (2011) J Phys Chem C 115:16764
68. Giustetto R, Levy D, Wahyudi O, Ricchiardi G, Vitillo JG (2011) Eur J Miner 23:449